

Autonomous and Decentralized Orbit Determination and Clock Offset Estimation of Lunar Navigation Satellites Using GPS Signals and Inter-satellite Ranging

Keidai Iiyama, Ryu Funase *The University of Tokyo*

BIOGRAPHY

Keidai Iiyama is a first year Ph.D. student at The University of Tokyo, Tokyo, and an incoming Ph.D. student at the Aeronautics and Astronautics Department at Stanford University from September, 2021. He received his B.S. degree (2019) and his M.S degree (2021) in Aerospace Engineering from The University of Tokyo.

Ryu Funase is an associate professor at The University of Tokyo. His research is on micro/nano satellites, navigation and control of spacecrafts, and spacecraft autonomy and intelligence.

ABSTRACT

The development of a robust navigation infrastructure in cis-lunar space is crucial for the coming new era of advanced lunar exploration. NASA has set a goal to develop an extensible and scalable lunar communication and navigation architecture called LunaNet. For the flexibility and robustness of the system, the architecture is desired to have an autonomous and decentralized operation capability. In this work, we propose a decentralized and autonomous state estimation algorithm for SmallSats that provides positioning, navigation, and timing service, each equipped with a GNSS receiver, a chip-scale atomic clock, and a steering antenna for inter-satellite communication. In our framework, each satellite individually estimates its own state and clock offset with a modified decentralized Schmidt Extended Kalman Filter by processing weak GNSS signal and inter-satellite range measurements. We also demonstrate that by deploying a total of 5 satellites on lunar frozen orbit and halo orbit, the PNT service area could be extended to regions where direct GNSS signals are not available, including the far side and pole regions of the moon.

I. INTRODUCTION

The development of robust navigation architecture in cis-lunar space is critical to support the advanced lunar missions in the coming decade. To meet this requirement, NASA has proposed a concept of an extensible and scalable lunar communication and navigation architecture called LunaNet [1]. LunaNet consists of satellites from various providers, including NASA, commercial industry, and academia, and will be operated in a dynamic and network-centric manner to provide networking services and positioning, navigation, and timing (PNT) services.

To provide an accurate PNT service, the position, velocity, and clock offset of the navigation satellites have to be estimated accurately. However, because the number of deep space ground stations is limited, continuous tracking and operation of all navigation satellites via ground stations could become infeasible as the system size grows. Therefore, autonomous state estimation of the navigation satellites is essential to reduce the operational cost and conflicts with other deep space missions. The autonomous state estimation capability will also improve the robustness of the navigation architecture.

Scalability and flexibility are also the core of the concept. To make the system flexible and extensible, it is desirable that autonomous state estimation of the navigation satellites is conducted in a decentralized manner. For scalability, using CubeSats as navigation satellites is also essential. With its low development and deployment cost, SmallSats could significantly increase the scalability and extensibility of the architecture. However, it is difficult to equip highly accurate atomic clocks on CubeSats due to its limited size and power availability. Therefore, the feasibility of using commercial chip-scale atomic clocks (CSACs), which have a much smaller size, power consumption, and cost but limited stability, must be carefully investigated.

Recently, several autonomous orbit determination methods in cis-lunar regions have been proposed. One major trend is to use inter-satellite ranging for autonomous interplanetary orbit determination, which is also known as liaison navigation [2, 3]. In regions where satellites are strongly affected by both Earth and Moon, the orbits of two satellites could be simultaneously determined using only the inter-satellite ranging between them by leveraging the asymmetry of the acceleration field. However,

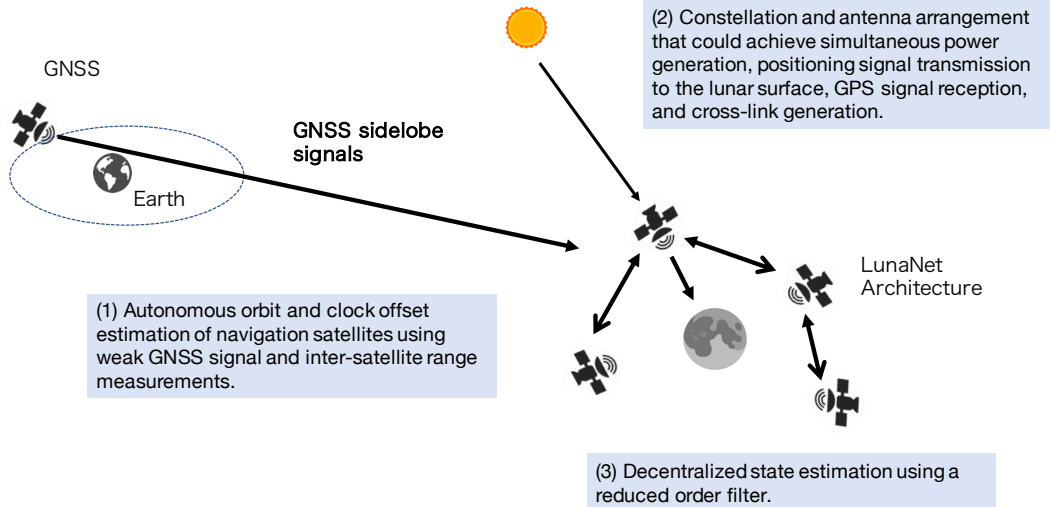


Figure 1: General Concept of the study

the liaison navigation alone could not provide sufficient clock offset estimation when clock stability is not sufficient due to observability problems. In addition, decentralized estimation is not considered in previous liaison research. Another trend is the usage of weak GNSS signals in lunar orbits [4, 5]. However, we could not leverage the observation data obtained by other navigation satellites when each satellite relies solely on individual GPS signal measurements, leading to limited state estimation accuracy.

With these in mind, the aim of this paper is to propose a decentralized and autonomous orbit determination and clock offset estimation algorithm for the lunar navigation satellites equipped with CSACs, and to demonstrate the achievable PNT performance that could be provided by the proposed navigation architecture. To the best of our knowledge, this paper is the first work to combine GPS weak signals measurement and intersatellite ranging to design a decentralized and autonomous navigation architecture in cis-lunar space with SmallSats. The key contribution of our work could be summarized as follows.

1. We propose a robust decentralized autonomous orbit determination and clock synchronization method that utilizes a modified decentralized Schmidt Extended Kalman Filter to process inter-satellite and GPS signal measurements with an orbital filter.
2. We propose an effective candidate of the initial constellation for the lunar navigation architecture, a combination of four halo orbiters and a lunar frozen orbiter. The concept of this constellation is to make the best use of the advantages of the halo orbit, which is the wide coverage and small amount of required fuel for deployment and station-keeping, while mitigating the relatively large orbit determination and clock estimation errors of the halo orbiters due to a small orbit change at the apolune by leveraging inter-satellite ranging with the frozen orbiter. We also show that by devising the antenna configuration, we could simultaneously achieve positioning signal transmission to the lunar surface, power generation, GPS signal reception, and inter-satellite ranging with a single GPS receiver and cross-link antenna on each satellite.
3. Furthermore, we analyze the achievable orbit determination error and clock offset estimation error of CSAC equipped SmallSats on halo orbits and frozen lunar orbits via detailed simulation.
4. Finally, we analyze the achievable navigation accuracy on the lunar surface and low lunar orbits via simulation. We demonstrate that the proposed lunar navigation architecture could effectively extend the positioning and timing service area to regions where direct GNSS observations are not available, such as the far side and pole of the moon.

The overview of this paper is summarized in Figure.1. At the time we are writing this abstract, we have already finished most of the works for 1,2,3 and working on 4.

II. DECENTRALIZED AUTONOMOUS STATE ESTIMATION

The position, velocity, time offset, and frequency offset of each satellite should be estimated. In this section, we propose a method to effectively estimate these states using a reduced order decentralized filter.

Decentralized orbit determination function based on inter-satellite range measurements is also employed on Beidou navigation satellites. The orbit determination algorithm of Beidou satellites is based on a method called ICEKF [6]. In this method, satellite i uses the current forecast estimate $\bar{X} = [\bar{X}_1, \dots, \bar{X}_N]$ and the observation matrix H_i for its own state only, and updates its own state estimate \hat{X}_i and the error covariance matrix P_{ii} . Then, the new estimate $\bar{X} = [\bar{X}_1, \dots, \bar{X}_N]$, where \bar{X}_i is replaced by \hat{X}_i , is transmitted to the next satellite $i + 1$ until the solution converges. However, since this method repeats the update based on the assumption that the state estimates of the other satellites are perfect, it often causes problems in convergence and error covariance estimation due to over-reliance on observations. Specifically, if the observation matrix for the ranging of satellite i and satellite j is described as $H = [H_i, H_j]$, then when calculating the Kalman gain HPH^T , the latter three terms of $HPH^T = H_i P_{ii} H_i^T + H_i P_{ij} H_j^T + H_j P_{ji} H_i^T + H_j P_{jj} H_j^T$ are ignored. In [6], several modifications are made to reduce the required number of iterations, but still, not all the terms of HPH^T are considered during the update.

To solve this problem, Schmidt Extended Kalman Filter is leveraged instead in our framework. In the Schmidt Kalman Filter, the total state is divided into two subsets: parameters that are actually estimated (the state of own satellites, denoted by x) and the parameters that only its variance is considered (the state of other satellites, denoted by y). In the algorithm, only the estimate of the former state is updated, but the effect of the latter variables is considered when calculating the covariance matrices and Kalman gain. The measurement update is as follows [7].

$$\begin{aligned}
\alpha_k &= H_k P_{xx_k}^- H_k^T + H_k P_{xy_k}^- J_k^T + J_k P_{yx_k}^- H_k^T \\
&\quad + J_k P_{yy_k}^- J_k^T + R_k \\
K_k &= (P_{xx_k}^- H_k^T + P_{xy_k}^- J_k^T) \alpha_k^{-1} \\
\hat{x}_k^+ &= \hat{x}_k^- + K_k (z_k - H_k \hat{x}_k^-) \\
P_{xx_k}^+ &= (I - K_k H_k) P_{xx_k}^- - K_k J_k P_{yx_k}^- \\
P_{xy_k}^+ &= (I - K_k H_k) P_{xy_k}^- - K_k J_k P_{yy_k}^- \\
P_{yx_k}^+ &= P_{yx_{k+1}}^{-T} \\
P_{yy_k}^+ &= P_{yy_k}^-
\end{aligned} \tag{1}$$

Unlike the ICEKF, the P_{xy} , P_{yy} are reflected in the calculation of α which is used when calculating the Kalman gain in Eq.1. This enables the estimation to take into account the effect of the state estimation error of other satellites.

In the time update, all states and covariances are updated as follows.

$$\hat{x}_{k+1}^- = \phi_{x_k} \hat{x}_k^+ \tag{2}$$

$$P_{xx_{k+1}}^- = \phi_{x_k} P_{xx_k}^+ \phi_{x_k}^T + Q_{x_k} \tag{3}$$

$$P_{xy_{k+1}}^- = \phi_{x_k} P_{xy_k}^+ \phi_{y_k}^T \tag{4}$$

$$P_{yx_{k+1}}^- = P_{yx_{k+1}}^{-T} \tag{5}$$

$$P_{yy_{k+1}}^- = \phi_{y_k} P_{yy_k}^+ \phi_{y_k}^T + Q_{y_k} \tag{6}$$

When using the Schmidt EKF algorithm in our problem setting, the following two factors have to be considered.

- The two satellites could exchange their estimated states during inter-satellite ranging.
- Continuous links among all satellites are not available. Therefore, the filtering algorithm also has to converge robustly under imperfect knowledge of the state estimates of other satellites.

With these two factors in mind, we modified the Schmidt EKF algorithm as follows.

Case 1: When satellite i, j are conducting inter-satellite ranging

1. Exchange \hat{x}^- and \hat{P}_{xx}^- information between the satellites, and replace the corresponding part of \hat{y}^- and \hat{P}_{yy}^- with the received value.
2. Update each other's estimates and covariance matrix according to Equation 1, and pass the updated \hat{x}^+ and \hat{P}_{xx}^+ to the other satellite.

- Each satellite propagates the covariance associated with itself to the next time according to equation (2) - equation (5). Return to 1.

Case 2: When satellite i is not conducting inter-satellite ranging with other satellites

- Since the estimates y , covariance P_{yy} , and observation matrix J_k for the other satellites are not known, set them as zero matrices. In addition, reset P_{xy} to zero to avoid inaccurate propagation of covariance matrices by the calculation of Eq. (4) and (5) using ϕ_y calculated from inaccurate y .
- Update only own estimates \hat{x}^+ and \hat{P}_{xx}^+ from observations using Eq. (1).
- Propagate the estimates and covariances to the next time according to equations (2) and (3). Return to Step 2.

III. CONSTELLATION AND ANTENNA ARRANGEMENTS

In this paper, a halo orbit is used for navigation satellite constellation considering the following advantages.

- By low-energy orbital transfer, satellites could be deployed with relatively low fuel consumption compared with low lunar orbits. Fuel consumption for station-keeping could also be kept low because of the high stability of the halo orbits.
- Halo orbits have excellent coverage of the far side and the pole of the moon, and its large orbit size enables it to provide positioning services in a wider area with a small number of satellites.
- Solar eclipses could be avoided by deploying the satellites into an orbit called synodic halo orbit, where the orbital period and the synodic period are in an integer ratio.

When considering the autonomous operation of the navigation architecture, there are the following advantages to add a satellite also on the frozen orbit.

- It is assumed that each navigation satellite is pointing the antenna on the PZ surface to the moon direction, and orienting its solar panel on the Y axis to the sun. When inter-satellite ranging is conducted between two halo orbiters with this orientation, the position of the other satellite shifts greatly in the body fixed frame of the satellite as shown in Fig.2. On the other hand, frozen orbiter direction in the body fixed frame circulates around the limited region around the PZ axis as shown in Figure 3, and it is easier to track from halo orbiters.
- The orbit and clock offset of the frozen orbiter could be estimated with high accuracy compared with halo orbiters, thanks to its larger geometric variation with respect to GPS satellites. The clock offset estimation error of the halo orbiter could be reduced by sharing information with the frozen orbiter.
- Diverse cross-link geometry could be obtained by conducting inter-satellite ranging between the frozen orbiter and halo orbiter, which leads to faster convergence and reduction of the orbit determination error for both halo orbiter and frozen orbiters.

The proposed hybrid constellation of halo and frozen orbits is shown in Figure. 4. In particular, 5:2 Synodic L2 north halo orbit is used, and four satellites are equally phased at $\Phi = 0^\circ, 90^\circ, 180^\circ, \text{ and } 270^\circ$. A single orbiter is deployed on a frozen orbit with orbit elements of $a = 6541 \text{ km}, e = 0.6, i = 56.2 \text{ deg}, \omega = 90 \text{ deg}$, taken from the work by Ely, et al. (2001) [8].

In order to achieve sun tracking, LNSS signal transmission, GNSS signal tracking, and inter-satellite ranging simultaneously, the attitude mode, arrangement of the antenna and solar array paddles are devised. The result is shown in Table.1.

Table 1: Antenna, SAP placement and attitude mode of navigation satellites

	Halo Orbit Satellite	Frozen Orbit Satellite
Attitude Mode	PZ Earth Pointing	PZ Moon Pointing
LNSS Tx Antenna	MZ (no steering)	PZ (no steering)
Earth GPS Rx Antenna	PZ (no steering)	PZ (with steering)
SST Tx,Rx Antenna	MZ (with steering)	PZ (with or no steering)
Solar Array Axis	PY, MY	PY, MY

IV. SIMULATION STUDY

1. Simulation Condition

For the dynamics of the spacecraft, the Earth, Sun and Moon gravity are taken into account, and the Earth's higher-order gravity term is considered up to the second-order, and the lunar higher-order gravity term is considered up to the eighth order for both

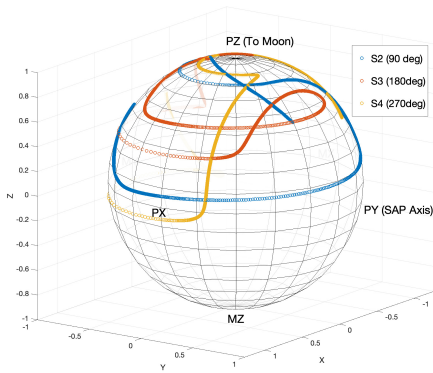


Figure 2: The transition of the direction to satellites at phase 90°, 180°, and 270° at the body fixed frame of a halo orbiter in phase 0° (for one orbital period).

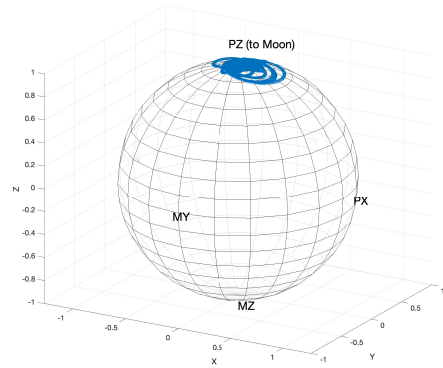


Figure 3: Transition of the direction to the frozen orbit on the fixed coordinate system of the halo orbiter in phase 0° (for one orbital period). Frozen orbiters are easier to track from halo orbiters.

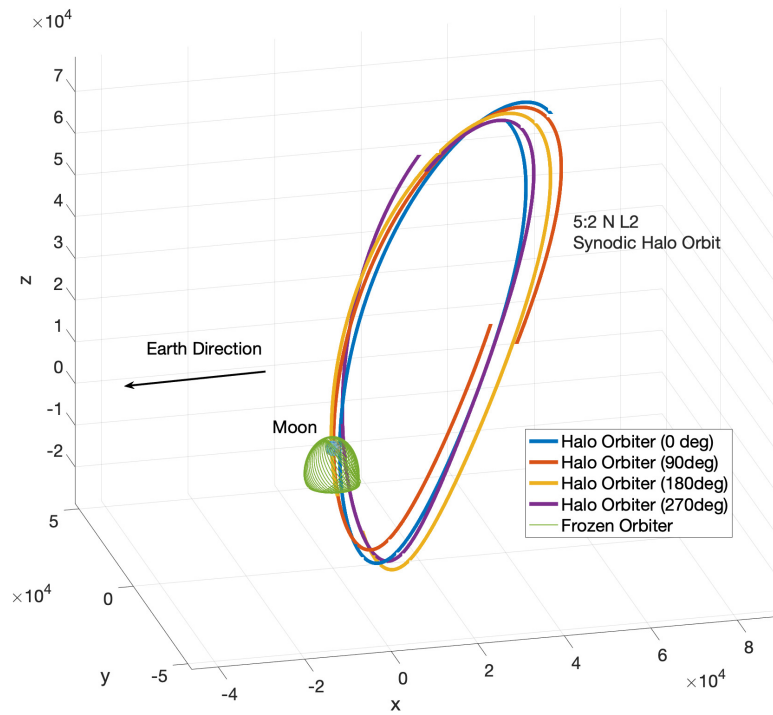


Figure 4: Hybrid constellation of halo orbiter and frozen orbiter

the true and estimated systems. To simulate the clock drift of CSAC, Allan variance of CSAC from MICROSEMI is used. The clock drift was modeled as a two-state Kalman Filter covariance model derived from the Allan variance parameters [9, 10].

In order to simulate the GPS signal in lunar orbits, it is necessary model the transmitter antenna patterns of the GPS satellites or the analysis of the sidelobe signal. We simulated the antenna pattern using the original data by Lockheed Martin [11] for Block IIR and IIR-M satellites, and the results of NASA’s GPS ACE project [12] for other blocks. An example of the simulated antenna pattern is shown in Fig.5.

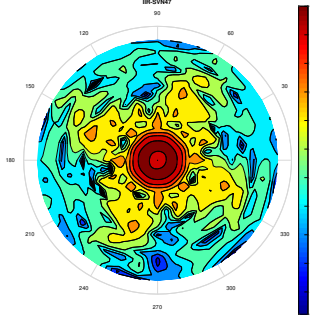


Figure 5: An example of the reconfigured GPS transmitter antenna pattern

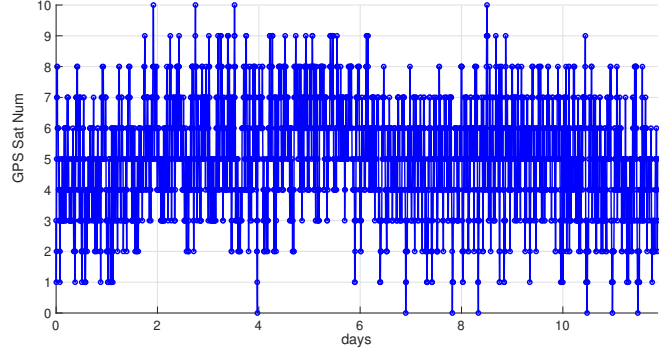


Figure 6: Number of GPS signals tracked at halo orbit

We assumed a GPS receiver with a maximum gain of 14 dBi and a half-width of 6 degrees, referring to [13]. It was assumed that GPS signals could be tracked when $C/N_0 > 15$. The change in the number of satellites tracked by the halo orbiter is shown in Figure 6. On average, 5.03 signals from GPS satellites were tracked from the halo orbiter and 5.16 signals from GPS satellites were tracked at the frozen orbiter.

The obtained pseudo-distance and pseudo-velocity were directly used as observables in the filter. The measurement error was calculated as thermal noise added by the Delay Lock Loop and Frequency Lock Loop for the range and range rate, respectively, which could be calculated as follows [14].

$$\sigma_{\rho_{DLL}} = \lambda_c \sqrt{\frac{B_n}{2C/N_0} \frac{1}{B_{fe} T_c} \left[1 + \frac{1}{TC/N_0} \right]} \quad (7)$$

$$\sigma_{\dot{\rho}_{FLL}} = \frac{\lambda_L}{2\pi T} \sqrt{\frac{4B_n}{C/N_0} \left[1 + \frac{1}{TC/N_0} \right]} \quad (8)$$

2. Results and Discussion

The results of the autonomous estimation over two orbital periods of the halo orbits using only GPS signals are shown in Fig.7 and 8. For the halo orbit, the estimation accuracy of both the position and velocity clocks decreased significantly around the apolune (0, 12, and 24 days), resulting in a maximum position error of about 500 m and a clock estimation error of about $1 \mu s$. This is because the orbit change rate becomes smaller near the apolune of the halo orbit, which reduces the sensitivity of the observation and the amount of information obtained. In the second cycle, the accumulation of covariance information reduces the estimation error.

Next, we consider using inter-satellite ranging measurements in addition to the GPS measurements. The timing of ranging and the selection of the cross-link pairs could vary, depending on the capacity of the communication system. At first, we assume that communication is possible when the distance between satellites is less than 4×10^4 km, and cross-links are only conducted between the frozen orbiter and the halo orbiters. The ranging error is set to 1 m. The transition of the cross-link pair satellite of the frozen-orbiter for this case is shown in Figure 9. The transition of the estimation error is shown in the following Figures 10 and 11.

The time average of the estimation errors during the second period for the two simulation cases are summarized in Table 2,3. Compared with using GPS alone, the position estimation error of the halo orbiter could be reduced by about 30m, and the clock

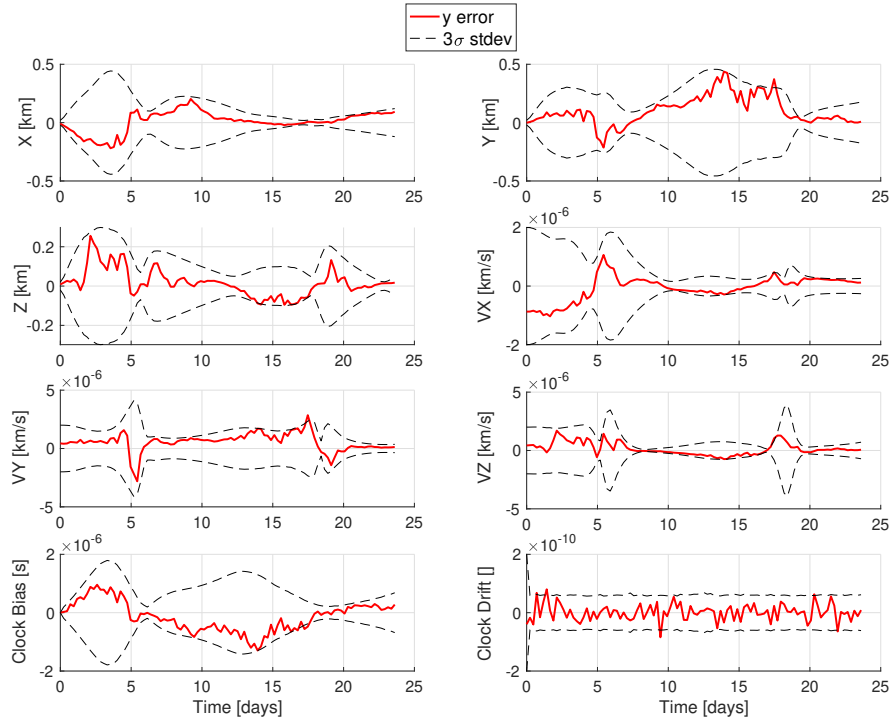


Figure 7: Estimation error of the halo orbiter at $\Phi = 0$ (using GPS signals only)

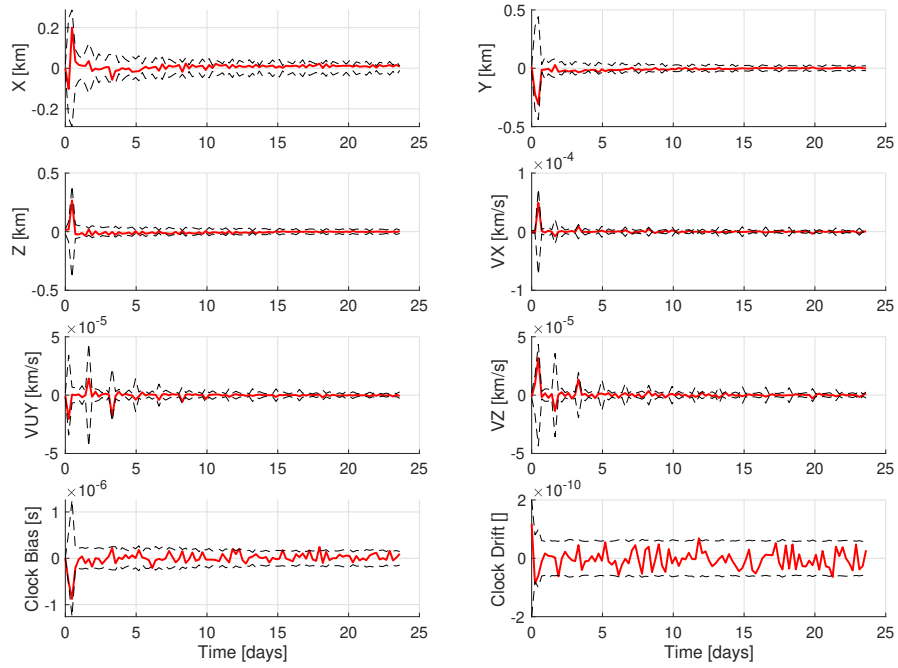


Figure 8: Estimation error of the frozen orbiter (using GPS signals only)

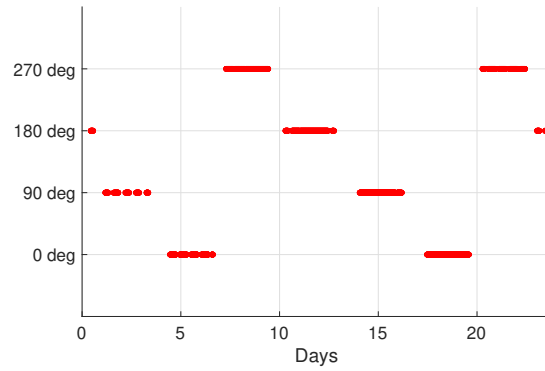


Figure 9: Ranging timing of frozen orbit satellite with each halo orbiters

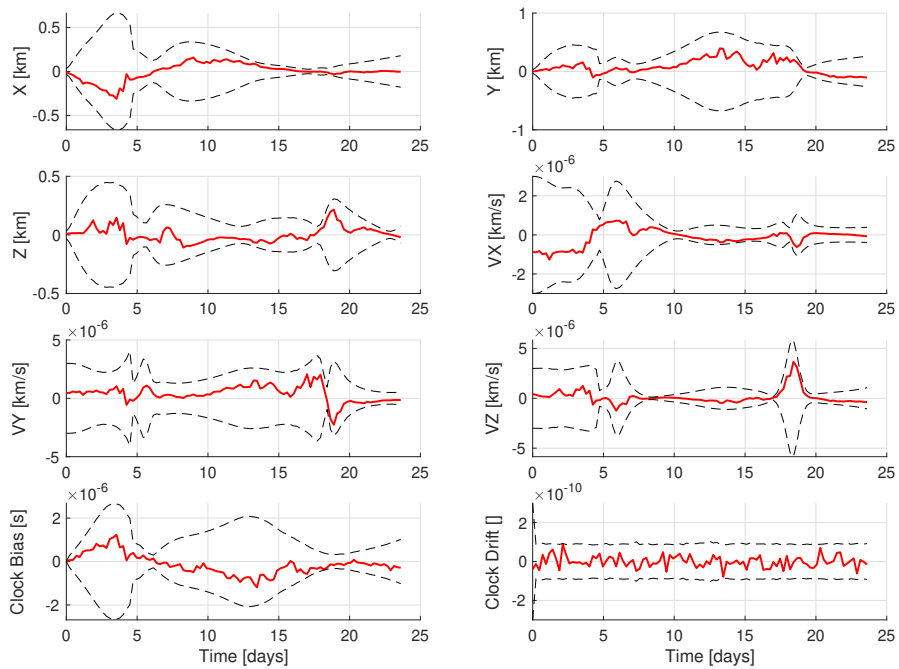


Figure 10: Estimation error of the halo orbiter at $\Phi = 0$ (using GPS signal + satellite crosslinks)

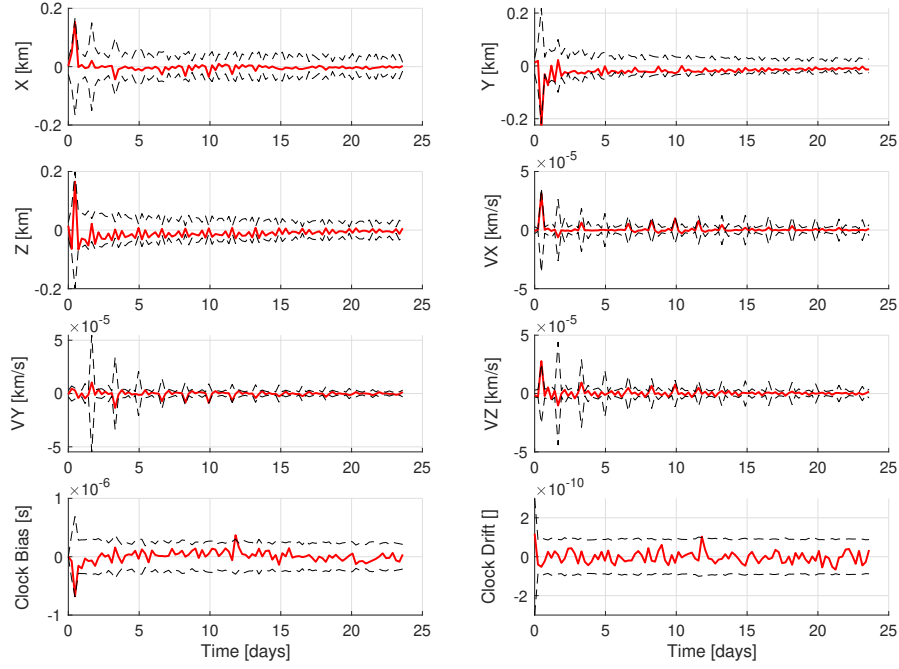


Figure 11: Estimation error of the frozen orbiter (using GPS signal + satellite crosslinks)

offset error could be reduced by about $0.1 \mu\text{s}$ by using inter-satellite ranging.

Table 2: Position Estimation Error (RMS) [m]

	GPS	GPS + Cross-links
Halo Orbiter ($\Phi=0$)	130.73	103.45
Frozen Orbiter	24.61	16.24

Table 3: Clock Offset Estimation Error [s]

	GPS	GPS + Cross-links
Halo Orbiter ($\Phi=0$)	3.54E-07	2.74E-07
Frozen Orbiter	0.84E-07	0.70E-07

V. CONCLUSIONS AND FUTURE WORK

In summary, we developed a decentralized and autonomous orbit determination and clock offset estimation algorithm for the lunar navigation satellites equipped with SmallSats. Weak GPS signal and inter-satellite ranging measurements are processed using the modified decentralized Schmidt Extended Kalman Filter. A hybrid constellation of lunar frozen orbit and halo orbit is proposed as an initial candidate for the navigation architecture, and its advantage for both autonomous state estimation and PNT service supply is stated. We analyzed the achievable orbit determination and clock offset estimation error and demonstrated that the usage of cross-links could reduce the state estimation error.

Planned future works for the final manuscript is as follows

- Analyze the PNT performance of the proposed hybrid constellation on the lunar surface and low lunar orbits.
- Consider additional error sources, such as station-keeping maneuvers and solar radiation pressure modeling errors.
- Test different halo orbit sizes, phasing of the satellites, and inter-satellite cross-link patterns for better performance.

REFERENCES

- [1] D. J. Israel, K. D. Mauldin, C. J. Roberts, J. W. Mitchell, A. A. Pulkkinen, L. V. D. Cooper, M. A. Johnson, S. D. Christe, and C. J. Gramling, "LunaNet: A Flexible and Extensible Lunar Exploration Communications and Navigation Infrastructure," *IEEE Aerospace Conference Proceedings*, 2020.

- [2] K. Hill and G. Born, "Autonomous Interplanetary Orbit Determination Using Satellite-to-Satellite Tracking," *Journal of Guidance, Control, and Dynamics*, vol. 30, no. 3, pp. 679–686, 2007. [Online]. Available: <http://arc.aiaa.org/doi/10.2514/1.24574>
- [3] K. A. Hill and G. H. Born, "Autonomous Orbit Determination from Lunar Halo Orbits Using Crosslink Range," *Journal of Spacecraft and Rockets*, vol. 45, no. 3, pp. 548–553, 2008. [Online]. Available: <http://arc.aiaa.org/doi/10.2514/1.32316>
- [4] V. Capuano, F. Basile, C. Botteron, and P. A. Farine, "GNSS-based Orbital Filter for Earth Moon Transfer Orbits," *Journal of Navigation*, vol. 69, no. 4, pp. 745–764, 2016.
- [5] V. Capuano, P. Blunt, C. Botteron, and P. A. Farine, "Orbital Filter Aiding of a High Sensitivity GPS Receiver for Lunar Missions," *Navigation, Journal of the Institute of Navigation*, vol. 64, no. 3, pp. 323–338, 2017.
- [6] Y. Wen, J. Zhu, Y. Gong, Q. Wang, and X. He, "Distributed orbit determination for global navigation satellite system with inter-satellite link," *Sensors (Switzerland)*, vol. 19, no. 5, 2019.
- [7] P. A. Ferguson and J. P. How, "Distributed Estimation and Control Technologies for Formation Flying Spacecraft," 2003.
- [8] T. A. Ely and E. Lieb, "CONSTELLATIONS OF ELLIPTICAL INCLINED LUNAR ORBITS PROVIDING POLAR AND GLOBAL COVERAGE," *AAS/AIAA Astrodynamics Specialists Conference*, vol. 1, pp. 1–13, 2001.
- [9] A. J. Van Dierendonck, J. B. McGraw, and R. G. Brown, "Relationship Between Allan Variances and Kalman Filter Parameters," *Sixteenth Annual Precise Time and Time Interval (PTTI) Applications and Planning Meeting*, p. 21, 1984.
- [10] T. Krawinkel and S. Schön, "Benefits of receiver clock modeling in code-based GNSS navigation," *GPS Solutions*, vol. 20, no. 4, pp. 687–701, 2016.
- [11] W. A. Marquis and D. L. Reigh, "The GPS Block IIR and IIR-M Broadcast L-band Antenna Panel: Its Pattern and Performance," *Navigation, Journal of the Institute of Navigation*, vol. 62, no. 4, pp. 329–347, 2015.
- [12] J. E. Donaldson, J. J. Parker, M. C. Moreau, D. E. Highsmith, and P. D. Martzen, "Characterization of on-orbit GPS transmit antenna patterns for space users," *Navigation, Journal of the Institute of Navigation*, vol. 67, no. 2, pp. 411–438, 2020.
- [13] A. Delépaut, P. Giordano, J. Ventura-Traveset, D. Blonski, M. Schönfeldt, P. Schoonejans, S. Aziz, and R. Walker, "Use of GNSS for lunar missions and plans for lunar in-orbit development," *Advances in Space Research*, vol. 66, pp. 2739–2756, 2020.
- [14] C. J. H. Elliott D. Kaplan, *Understanding GPS. Principles and applications*, 1997, vol. 59, no. 5. [Online]. Available: <http://linkinghub.elsevier.com/retrieve/pii/S1364682697833378>